Avalanches in Strained Amorphous Solids: Does Inertia Destroy Critical Behavior?

K. Michael Salerno, Craig E. Maloney, and Mark O. Robbins

Phys. Rev. Lett. **109**, 105703 — Published 6 September 2012

DOI: 10.1103/PhysRevLett.109.105703

Avalanches in Strained Amorphous Solids: Does Inertia Destroy Critical Behavior?

K. Michael Salerno, Craig E. Maloney, and Mark O. Robbins
Department of Physics and Astronomy, Johns Hopkins University, Baltimore, Maryland 21218 USA and Department of Civil Engineering, Carnegie Mellon University, Pittsburgh, Pennsylvania 15213
(Dated: July 27, 2012)

Simulations are used to determine the effect of inertia on athermal shear of amorphous two-dimensional solids. In the quasistatic limit, shear occurs through a series of rapid avalanches. The distribution of avalanches is analyzed using finite-size scaling with thousands to millions of disks. Inertia takes the system to a new underdamped universality class rather than driving the system away from criticality as previously thought. Scaling exponents are determined for the underdamped and overdamped limits and a critical damping that separates the two regimes. Systems are in the overdamped universality class even when most vibrational modes are underdamped.

PACS numbers: 64.60.av,62.20.F-,45.70.Ht,61.43.Bn

Many slowly driven physical systems exhibit long quiescent periods punctuated by rapid avalanches [1–3]. Phenomena as diverse as earthquakes, Barkhausen noise in magnetic materials, dislocation cascades in single crystal microcompression and fluid interface depinning display power law avalanche statistics in seismicity, acoustic emission, slip, stress drop or interface advance [4–11]. These power laws reflect a non-equilibrium critical transition at the onset of motion.

This Letter addresses a fundamental question about the effect of inertia on such critical behavior. Power law scaling has normally been observed in overdamped systems. Studies of underdamped systems [2, 12–15] or stress overshoot models designed to mimic inertia [16–19], suggest that inertia drives systems away from the critical point. In sandpiles, the onset of motion appears to become a hysteretic first-order transition [14]. In the Burridge-Knopoff model, inertia leads to a growing importance of non-critical, system spanning events [15]. The conclusion that inertia destroys critical behavior seems at odds with the observation of power law scaling in earthquakes and laboratory compression tests [4, 8, 9], where seismic waves and acoustic emission indicate that the systems are underdamped.

Here, quasistatic simulations of sheared amorphous solids are performed over a full range of damping rates. The results reveal a rich phase diagram. Different universality classes describe the overdamped and underdamped limits, but both are described by critical finite-size scaling relations. The transition between the two limits occurs at a fixed damping rate that appears to have its own scaling behavior. Overdamped scaling extends to surprisingly small damping rates, where nearly all vibrational modes are underdamped. The power law describing underdamped avalanches is close to the Gutenberg-Richter law and there is an excess of large events that is similar to that seen in individual fault systems [20].

Since we are interested in the general question of how inertia affects critical behavior, we choose a simple model system. Work by Dahmen et al. suggests mean-field behavior extends to two dimensions [18, 19] and we consider a two-dimensional binary mixture of disks that has been widely studied as a model amorphous system [21–25]. The disks may represent atoms, grains, bubbles, colloids or volume elements of a deforming fault zone. We focus on the athermal limit for three reasons: First, it allows clear identification of small avalanches. Second, other work indicates that temperature may drive systems away from criticality [25]. Finally, macroscopic systems, like fault zones or the photoelastic disks commonly used in experiments[26, 27], are in the athermal limit.

Particles interact via the Lennard-Jones (LJ) potential, $U(\mathbf{r}) = 4u_0[(a_{ij}/r)^6 - (a_{ij}/r)^{12}]$ where r is the magnitude of the vector $\mathbf{r}$ between two disks and the species i,j are of two types, A and B. To prevent crystallization, the disks have different diameters $a_{AA} = 5/3\ a_{BB} = a$ and $a_{AB} = 4/5\ a$. The LJ energy and force are taken smoothly to zero at $r_c = 1.5a_{ij}$ using a polynomial fit starting at $1.2a_{ij}$ [28]. Both disk types have mass m and the number ratio $N_A/N_B = (1+\sqrt{5})/4$. The depth of the potential u_0 sets the energy scale of interactions. The natural unit of time is $t_{LJ} = \sqrt{ma^2/u_0}$.

Initial states are prepared as in Ref. [28], but, as there, the protocol has little effect on steady state shear. After annealing, the system contains $N \sim 10^3 - 10^6$ disks in a square unit cell with edge $L = 55a$ to $875a$ and periodic boundary conditions. The density $\rho = 1.38a^{-2}$ and the pressure is near zero. A pure shear strain ϵ is applied to the system by changing the length of the periodic simulation cell while holding the area constant so that $L_x = Le^{-\epsilon}$ and $L_y = Le^{\epsilon}$. The strain rate $|\dot{\epsilon}| < 10^{-6}t_{LJ}^{-1}$ between avalanches was adjusted for each L to ensure simulations were in the quasistatic limit where results depend only on strain interval and not independently on time. When an increase in kinetic energy indicated the onset of plastic deformation, $|\dot{\epsilon}|$ was reduced to zero to allow the avalanche to evolve without external perturbation. Shearing resumed after the kinetic energy dropped below 1% of the background value during shear.

In order to model the athermal limit, the kinetic en-

ergy released during avalanches must be removed by some damping mechanism. A viscous drag force was applied to each disk, $\mathbf{F}_{drag} = -\Gamma m\mathbf{v}$ where $\mathbf{v}$ is the non-affine velocity. As the dissipation rate Γ decreases, the dynamics changes from overdamped to underdamped (inertial) dynamics. Vibrational modes with frequency $\omega > \Gamma$ are underdamped, and it is useful to compare Γ to the root mean squared or Einstein frequency $\omega_E \equiv \sqrt{\langle\omega^2\rangle} = 17t_{LJ}^{-1}$.

We focus on the steady state achieved after plastic rearrangements have erased memory of the initial state ($\epsilon > 7\%$). While the system is trapped in a local energy minimum, work done by the applied strain leads to a nearly linear rise in potential energy and shear stress σ_s. When the minimum becomes unstable, there is a rapid avalanche of activity that leads to a sharp drop by E in energy and by $\Delta\sigma_s$ in shear stress. In the overdamped limit, the system is trapped in the next local energy minimum. When damping is reduced, inertia can carry the system over subsequent energy barriers to reach lower energy states. One dramatic consequence is that the mean potential energy sampled by systems decreases by 30% as Γ decreases. Indeed, there is almost no overlap between the ranges of potential energy sampled for the three damping rates studied in detail below, $\Gamma t_{LJ} = 1$, 0.1 and 0.001.

A sum rule requires that the energy and stress drops in large events are proportional [29]. We find that this relation breaks down for small events and that considering both quantities facilitates identification of the critical region. To simplify comparison we rescale the stress drop by a constant factor to give a corresponding energy $S \equiv \Delta\sigma_s L^2 \langle\sigma_s\rangle / 4\mu$, where $\langle\sigma_s\rangle$ is the mean shear stress, μ is the shear modulus and $\langle\sigma_s\rangle / 4\mu \approx 0.02$ for all Γ and L. To quantify the distributions of event sizes, we define the event rates $R(S, L)$ and $R(E, L)$ as the number of events of energy S or E per unit energy and unit strain in a system of size L.

Figure 1 shows $R(S, L)$ for different L in the overdamped ($\Gamma t_{LJ} = 1$) and underdamped ($\Gamma t_{LJ} = 0.001$) limits. In contrast to other slowly driven systems that exhibit power law avalanche distributions [10, 11], the number of small events does not scale linearly with the system size, L^2. The rates for different L collapse when scaled by L^γ with $\gamma = 1.2$ and 1.3 for overdamped and underdamped systems, respectively. This implies that as L increases large events suppress small events either by changing the local configurations so small events are less likely to occur, or by increasing the probability that the same local configuration will produce a large avalanche.

The distributions for both overdamped and underdamped systems saturate at low S and decrease as a power law $R(S, L) \propto S^{-\tau}$ for $S > 0.3u_0$. The power laws are different, indicating that inertia changes the universality class. For each Γ, results for each L follow the power law up to a maximum size that increases with L

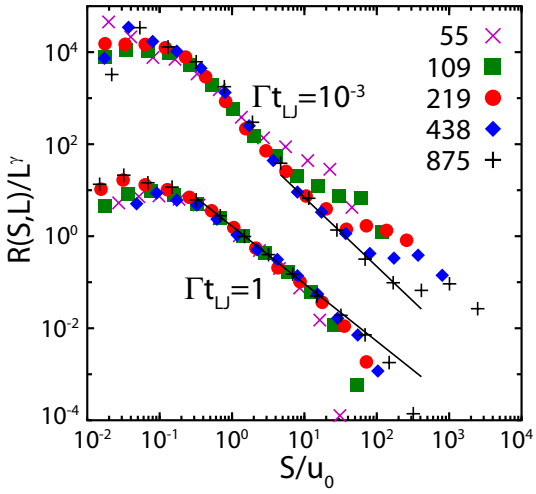

FIG. 1: Scaling of $R(S, L)$ with S for overdamped, $\Gamma t_{LJ} = 1$, systems with $\gamma = 1.3$ (lower curves) and underdamped, $\Gamma t_{LJ} = 0.001$, systems with $\gamma = 1.2$ (upper curves). Underdamped curves are multiplied by 100 to prevent overlap, symbols indicate L/a and symbol size is larger than statistical errors. Lines indicate the power laws obtained from finite-size scaling fits (Table I).

because larger systems allow larger avalanches. For the overdamped case, there is a simple monotonic drop in R at large S. The underdamped behavior is unusual because there is a plateau at large S, followed by a rapid drop. It is interesting to note that similar plateaus are observed in the distribution of earthquakes from individual fault systems [20].

The slope of curves in Fig. 1 can be used to estimate the power law exponent τ, but it is difficult to know where the critical scaling regime starts and ends. More accurate critical exponents are obtained using finite-size scaling methods [30] that focus on the scaling of large events. The distributions for both S and E are assumed to obey the finite-size scaling ansatz:

$$R(X, L) = L^\beta g(X/L^\alpha) \quad , \tag{1}$$

where X stands for S or E, the size of the largest events scales as L^α, and g is an unknown scaling function. The form of $g(y)$ at large y may depend on the boundary conditions used, but the scaling exponents do not [30].

Equation 1 produces power law scaling for $X << L^\alpha$ if $g(y) \propto y^{-\tau}$ for $y << 1$. One finds $R(X, L) \propto L^\gamma X^{-\tau}$ with $\gamma = \beta + \alpha\tau$. We can derive another scaling relation between exponents using the fact that the total energy dissipated per unit strain is $L^d \langle\sigma_s\rangle$ with dimension $d = 2$. The dissipated energy must also equal the sum of E or S over all avalanches. Integrating $XR(X, L)$ using Eq. 1, one finds that $\beta + 2\alpha = d$ as long as the integral of $yg(y)$ is well-defined.

As shown in Figure 2 excellent finite-size scaling collapses are obtained for E and S in both overdamped

($\Gamma = 1$) and underdamped ($\Gamma = 0.001$) limits. Values of α, β, γ and τ (Table I) were determined separately and then checked for consistency with the above scaling relations. A key feature of the underdamped results is that the plateaus for large events at different L collapse onto common curves. Thus the avalanche statistics are consistent with critical scaling even if the form of the scaling function is unusual.

As the event size decreases, results for each L follow the scaling function g for the given Γ until events are too small to be in the scaling regime. Analysis of the curves shows that this corresponds to S and E of order u_0. This is the energy of a single bond and analysis of events with much lower energy shows they are qualitatively different. Additional evidence that they are not in the critical regime comes from the sharply different behavior of S and E. Results for S tend to saturate for $S < u_0$, while results for E cross over to power law scaling with a lower exponent that changes slightly with L.

Previous studies have only considered the overdamped limit and used system sizes $L \leq 109$ [21, 29, 31, 32]. For these systems most events are in the noncritical scaling regime, $E < u_0$, explaining variations in the reported values of α [21, 29] and why some papers concluded there was no critical behavior [31, 32]. Values of the scaling exponent τ have not been reported in previous studies of sheared amorphous solids [21–23, 29] , but τ has been studied for a simpler lattice model by Dahmen et al. [19]. Their results suggest that τ has a mean-field value of 1.5 for all d in overdamped systems [19]. Our result of 1.25 is lower than this prediction, but substantially higher than the values of $\tau < 1$ that would be inferred from the noncritical power law region at small E in Fig. 2.

We now examine the transition between overdamped and underdamped limits as Γ varies. Given the large difference in α for the two cases, the scaling of large events will change sharply with Γ. A useful measure of the largest events is the ratio $\langle S^2 \rangle / \langle S \rangle$ [33]. As shown in Fig. 3(a), results for $\langle S^2 \rangle / \langle S \rangle L^\alpha$ at all L collapse onto a universal curve with the overdamped $\alpha = 0.9$ at large Γ. Separate simulations using the energy minimization ($\Gamma t_{LJ} \to \infty$) algorithm of many previous studies [21–23] were statistically indistinguishable from results for $\Gamma t_{LJ} \geq 1$. As Γt_{LJ} decreases from 1 to 0.1, the mean avalanche size increases in the same way for all L, indicating that α remains constant and the system is in the same universality class. Since $\omega_E t_{LJ} = 17$, systems remain in the overdamped universality class even when almost all vibrational modes are underdamped. The key factor is not whether modes are overdamped but whether inertia can carry the system over the next energy barrier in the energy landscape. A small Γ can trap the system in the nearest minimum if the difference in successive energy barriers is small and/or the path in phase space to the next barrier is complicated.

Fig. 3(b) shows that the underdamped $\alpha = 1.55$ collapses results for different L when $\Gamma t_{LJ} \leq 0.01$. For the simple viscous drag $-\Gamma m v$ employed here, the system is always overdamped at wavelengths larger than a length of order c/Γ, where $c = 3.4a/t_{LJ}$ is the shear velocity. One may ask whether the avalanche distribution would always exhibit overdamped behavior on lengths larger than this scale, which is comparable to our largest system sizes when $\Gamma t_{LJ} \leq 0.01$. We see no evidence of such a crossover at larger Γ, but stronger evidence is obtained by considering other thermostats. A viscous drag is only appropriate for systems with an inertial reference frame, such as photoelastic disks on a substrate

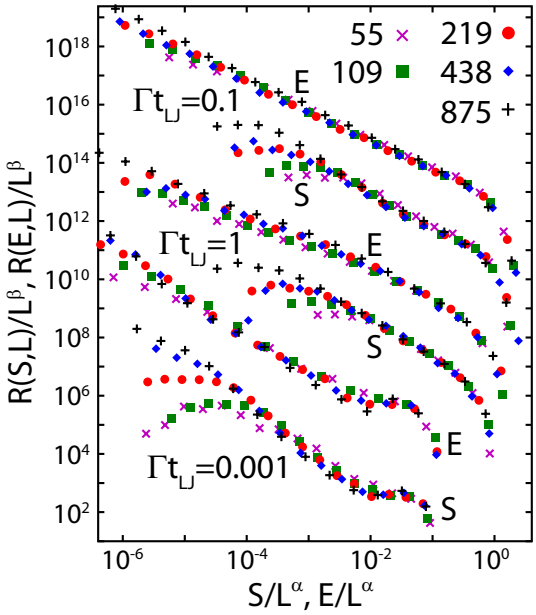

FIG. 2: (a) Finite-size scaling collapse of $R(S, L)$ and $R(E, L)$ for overdamped systems ($\Gamma t_{LJ} = 1$), underdamped systems ($\Gamma t_{LJ} = 0.001$) and critically damped systems ($\Gamma t_{LJ} = 0.1$) using the exponents in Table I. Statistical errors are smaller than the symbols and successive curves are shifted up by 2 or 3 decades to prevent overlap.

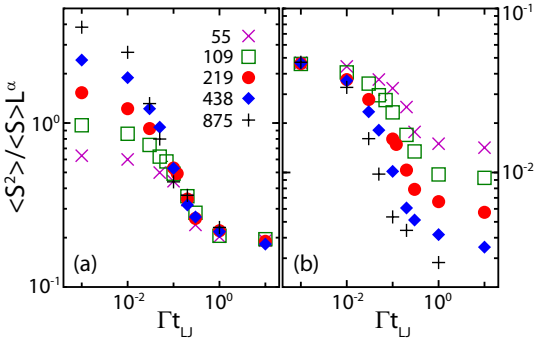

FIG. 3: Size of stress drops normalized by L^α plotted against (a) Γt_{LJ} with $\alpha = 0.9$ and (b) $\Gamma L/c$ with $\alpha = 1.55$. Statistical errors are comparable to the symbol size.

Γ	τ	α	β	γ
1.0	1.25 ± 0.05	0.9 ± 0.05	0.2 ± 0.1	1.3 ± 0.05
0.1	1.0 ± 0.05	0.9 ± 0.05	0.3 ± 0.1	1.2 ± 0.05
0.001	1.5 ± 0.1	1.55 ± 0.1	-1.1 ± 0.1	1.2 ± 0.1

TABLE I: Scaling exponents determined for overdamped ($\Gamma = 1$) and underdamped ($\Gamma = 0.001$) limits and at the transition between them $\Gamma = 0.1$. Quoted values satisfy the scaling relations $\beta + 2\alpha = d$ and $\gamma = \beta + \alpha\tau$ and errorbars are estimated from the quality of finite-size scaling collapses for E and S using other Γ and moments.

[26, 27]. In isolated disordered solids dissipation mechanisms must be Galilean-invariant and only damp *relative* velocities. In this case, long wavelength modes are always underdamped [34]. We have also performed simulations with the Galilean invariant thermostats described in Refs. [28, 35]. As illustrated in the supplemental material, these thermostats give the same avalanche distributions as a viscous drag in both the overdamped and underdamped limits. Moreover, the crossover between the two limits occurs over a comparable range of Γ. We thus conclude that for small Γ the power law distribution of avalanches is only cut off by the system size and not c/Γ.

The results in Fig. 3(a) show that there is a change in scaling at $\Gamma t_{LJ} \approx 0.1$. Figure 2 also presents a finite-size scaling collapse of avalanche distributions for this critical damping, which has its own exponents (Table I). The results for E follow a power law with $\tau = 1$ over 6 decades or more. We have found similar scaling for intermediate damping with Galilean invariant thermostats, for different interaction potentials, for simple shear, and in preliminary studies of 3D systems. This suggests that $\Gamma t_{LJ} = 0.1$ represents a multicritical point separating regions that flow to underdamped and overdamped fixed points.

In conclusion, introducing inertia does not destroy critical scaling of avalanches in quasistatic shear of disordered solids. Systems continue to be in the overdamped universality class even when most vibrational modes are underdamped. Only a small amount of damping is needed to prevent inertia from carrying systems over sequential energy barriers, implying that the difference between energy barriers is small or the path between them complex.

Below a critical damping rate a new universality class corresponding to the underdamped limit is identified. While our system lacks the complexity found in earthquake faults, it is interesting to note that τ is close to the value of ~ 1.6 for laboratory compression tests [8, 9] and the Gutenberg-Richter law [20]. In addition, the distribution of earthquakes for a given fault system typically has an excess of large events that is similar to the plateau seen in Figs. 1 and 2 [20].

Different scaling exponents are observed at the critical damping rate that separates overdamped and underdamped limits, indicating that it is a multicritical point. The scaling exponents in all three regimes (Table I) satisfy the scaling relations $\beta + 2\alpha = d$ and $\gamma = \beta + \alpha\tau$. The hyperscaling relation $\gamma = d$ is violated in all cases. The number of avalanches at a given energy rises less rapidly than system size ($\gamma < d$), indicating that small events are suppressed by the larger events in bigger systems. Exponents obtained from finite-size scaling of the distribution of energy and stress drops are consistent. However, there is a long power law tail in $R(E, L)$ at small E with a size dependent exponent and system-size independent cutoff. This tail appears to have dominated previous scaling studies using smaller systems [21, 29, 31, 32, 36]

We thank Karin Dahmen for useful discussions. This work was supported by the National Science Foundation under grants DMR-10046442, CMMI-0923018, and OCI-108849.

[1] J. Sethna, K. Dahmen, and C. Myers, Nature **410**, 242 (2001).
[2] D. S. Fisher, Phys. Rev. B **31**, 1396 (1985).
[3] P. Bak, C. Tang, and K. Wiesenfeld, Phys. Rev. Lett. **59**, 381 (1987).
[4] B. Gutenberg and C. F. Richter, Bulletin of the Seismological Society of America **34**, 185 (1944).
[5] P. A. Houle and J. P. Sethna, Phys. Rev. E **54**, 278 (1996).
[6] E. Vives, I. Ràfols, L. Mañosa, J. Ortín, and A. Planes, Phys. Rev. B **52**, 12644 (1995).
[7] S. Brinckmann, J.-Y. Kim, and J. R. Greer, Phys. Rev. Lett. **100**, 155502 (2008).
[8] M. C. Miguel, A. Vespignani, S. Zapperi, J. Weiss, and J.-R. Grasso, Nature **410**, 667 (2001).
[9] M. Zaiser, Adv. Phys. **55**, 185 (2006).
[10] N. Martys, M. O. Robbins, and M. Cieplak, Phys. Rev. B **44**, 12294 (1991).
[11] H. Ji and M. O. Robbins, Phys. Rev. B **46**, 14519 (1992).
[12] C. P. C. Prado and Z. Olami, Phys. Rev. A **45**, 665 (1992).
[13] G. A. Held, D. H. Solina, D. T. Keane, W. J. Haag, P. M. Horn, and G. Grinstein, Phys. Rev. Lett. **65**, 1120 (1990).
[14] H. M. Jaeger, C.-h. Liu, and S. R. Nagel, Phys. Rev. Lett. **62**, 40 (1989).
[15] J. M. Carlson and J. S. Langer, Phys. Rev. Lett. **62**, 2632 (1989).
[16] R. Maimon and J. M. Schwarz, Phys. Rev. Lett. **92**, 255502 (2004).
[17] M. C. Marchetti, PRAMANA **64**, 1097 (2005).
[18] K. A. Dahmen, Y. Ben-Zion, and J. T. Uhl, Phys. Rev. Lett. **102**, 175501 (2009).
[19] K. Dahmen, Y. Ben-Zion, and J. T. Uhl, Nature Physics **7**, 554 (2011).
[20] C. Scholz, *The mechanics of earthquakes and faulting* (Cambridge University Press, 2002).
[21] C. Maloney and A. Lemaître, Phys. Rev. Lett. **93**, 016001 (2004).

[22] N. P. Bailey, J. Schiøtz, A. Lemaître, and K. W. Jacobsen, Phys. Rev. Lett. **98**, 095501 (2007).
[23] H. G. E. Hentschel, S. Karmakar, E. Lerner, and I. Procaccia, Phys. Rev. Lett. **104**, 025501 (2010).
[24] A. Lemaître and C. Caroli, Phys. Rev. E **76**, 036104 (2007).
[25] S. Karmakar, E. Lerner, I. Procaccia, and J. Zylberg, Phys. Rev. E **82**, 031301 (2010).
[26] R. P. Behringer, K. E. Daniels, T. S. Majmudar, and M. Sperl, Phi. Trans. R. Soc. A **366**, 493 (2008).
[27] N. W. Hayman, L. Ducloué, K. L. Foco, and K. E. Daniels, Pure Appl. Geophys. **168**, 2239 (2011).
[28] C. E. Maloney and M. O. Robbins, Journal of Physics: Condensed Matter **20**, 244128 (2008).
[29] E. Lerner and I. Procaccia, Phys. Rev. E **79**, 066109 (2009).
[30] V. Privman, *Finite size scaling and numerical simulation of statistical systems* (World Scientific, 1990).
[31] S. Tewari, D. Schiemann, D. J. Durian, C. M. Knobler, S. A. Langer, and A. J. Liu, Phys. Rev. E **60**, 4385 (1999).
[32] T. Hatano, Phys. Rev. E **79**, 050301 (2009).
[33] We checked that higher moment ratios give the same scaling. The mean size $\langle S \rangle$ is not well-defined because the number of small events diverges for $\tau \geq 1$.
[34] L. Landau, E. Lifshitz, A. Kosevich, and L. Pitaevskiĭ, *Theory of Elasticity*, Theoretical Physics (Butterworth-Heinemann, 1986).
[35] P. J. Hoogerbrugge and J. M. V. A. Koelman, Europhys. Lett. **19**, 155 (1992).
[36] C. E. Maloney and A. Lemaître, Phys. Rev. E **74**, 016118 (2006).